DYNAMIC CHARACTERISTICS OF STRUCTURE TO STRUCTURE INTERACTION THROUGH SURFACE LAYER

by

Tomoyuki Inukai[I], Kenji Miura[I] and Takao Nishikawa[II]

SYNOPSIS

A method to analyze the effects of Dynamic Cross Interaction on the dynamic behaviors of embedded structures was presented. The method deals with two rigid structures problem by applying the three-dimensional wave propagation theory. By varying embedded depth, distance between structures and location of structures, many case studies were conducted.

INTRODUCTION

Dynamic behavior of embedded structure is fairly affected by the interaction between the side wall of structure and the surface layer. When a structure is embedded near one structure, radiational waves of one structure act on the other structure as incident waves. Dynamic characteristics of these structures become more complex compared to the single structure problem, because the influence of Dynamic Cross Interaction (DCI) should be induced. The analytical model consists of two rigid structures of cylindrical shape embedded into the surface layer. The analysis is performed by application of the three-dimensional wave propagation theory. To simplify the analysis the vertical displacement of the surface layer was neglected. The input ground motion $Ug \cdot e^{i\omega t}$ was applied on the bed rock in x-direction as shown in Fig. 1.

DISPLACEMENTS OF SURFACE LAYER

The displacements of the surface layer, expressed in the cylindrical coordinates $(r^{(I)}, \theta^{(I)}, z)$, are as follows;

$$\begin{aligned} u(r^{(I)},\theta^{(I)},z) &= u_C^{(I)}(r^{(I)},\theta^{(I)},z) + u_C^{(II)*}(r^{(II)},\theta^{(II)},z) + u_p(\theta^{(I)},z) \\ v(r^{(I)},\theta^{(I)},z) &= v_C^{(I)}(r^{(I)},\theta^{(I)},z) + v_C^{(II)*}(r^{(II)},\theta^{(II)},z) + v_p(\theta^{(I)},z) \end{aligned} \quad (1)$$

where u,v = total displacement of surface layer in $r^{(I)}$ and $\theta^{(I)}$ direction, respectively; $u_c^{(j)}, v_c^{(j)}$ = displacement caused by the radiational waves of Structure-(j) shown in coordinates $(r^{(j)},\theta^{(j)},z)$, (j=I or II); $u_c^{(II)*}, v_c^{(II)*}$ = values transformed $u_c^{(II)}$ and $v_c^{(II)}$ into coordinates $(r^{(I)},\theta^{(I)},z)$; u_p, v_p = displacements caused by shear wave traveling in z-direction independent of structures. And $u_c^{(j)}$ and $v_c^{(j)}$ include unknown integral constants.

Assuming that the rigid structures are vibrating with the rocking angles $\Phi_X^{(j)} \cdot e^{i\omega t}$ and $\Phi_Y^{(j)} \cdot e^{i\omega t}$ in x and y-direction, respectively, the continuity conditions of displacements between the side walls of structures and the surface

---

I. Research Associate, Dept. of Architectural Engineering, Tokyo Metropolitan University, Tokyo, Japan
II. Associate Professor, ditto

layer should be considered. The equations of boundary problem for Structure-I as follows;

$$u_C^{(I)}(a^{(I)},\theta^{(I)},z) + u_C^{(II)*}(R^{(II)},\theta^{(II)},z) + u_p(\theta^{(I)},z) = u_S^{(I)}(\theta^{(I)},z)$$
$$v_C^{(I)}(a^{(I)},\theta^{(I)},z) + v_C^{(II)*}(R^{(II)},\theta^{(II)},z) + v_p(\theta^{(I)},z) = v_S^{(I)}(\theta^{(I)},z) \quad (2)$$

in which $u_S^{(I)}, v_S^{(I)}$ = displacements of side wall of Structure-I; $R^{(II)},\theta^{(II)}$ = values presented side wall of Structure-I $(a^{(I)},\theta^{(I)})$ in the coordinates $(r^{(II)},\theta^{(II)})$. Since $(R^{(II)},\theta^{(II)})$ in Eq. 2 have one to one correspondence to $\theta^{(I)}$, Eq. 2 are considered to be a function of $\theta^{(I)}$ and z. Similarly, the boundary equations for Structure-II are expressed as a function of $\theta^{(II)}$ and z. Solving the equations by expanding $(u_C^{(II)*}, v_C^{(II)*})$ and $(u_C^{(I)*}, v_C^{(I)*})$ in the Fourier series, the integral constants are obtained as a function of $\Phi_X^{(j)}, \Phi_Y^{(j)}$ and Ug. Substituting these integral constants into Eq. 1, the displacements are given by a function of $\Phi_X^{(j)}, \Phi_Y^{(j)}$ and Ug.[1)]

ROCKING MOTIONS OF RIGID STRUCTURES AND DCI FACTORS

The rocking moments in x and y-direction due to the surface layer acting on the side walls of the structures are obtained by using the above mentioned integral constants. Assuming that the rigid structures have no sliding against the bed rock and the rocking axis in each direction coincides the base of structure, the equations of rocking motion are derived as follows;

$$[I\theta]\{\Phi\} = -[F]\{\Phi\} + \frac{1\pi}{2H}\left(\frac{\omega}{\omega g}\right)^2\{G\}Ug + \{Iu\}Ug \quad (3)$$

where $[I\theta],\{Iu\}$ = matrix and vector relative to moment of inertia and force of inertia, respectively; ωg = lowest natural frequency of surface layer; $\{\Phi\} = \{\Phi_X^{(I)},\Phi_Y^{(I)},\Phi_X^{(II)},\Phi_Y^{(II)}\}^T$ vector of rocking angle; $[F] = [f_{ik}]_{4\times4}$ matrix of DCI factors show frequency properties of reactive moments; $\{G\} = \{g_1,g_2,g_3,g_4\}^T$ vector of DCI factors show frequency properties of forcing moments. For example, f_{13} shows the dynamic characteristics of reactive moment acting on Structure-I in x-direction caused by the rocking motion of Structure-II in x-direction. In the static case, Fig. 2 shows the comparison of DCI factors with Tajimi's solution[2)] that are the factors of the single structure problem ($l/a = \infty$). In the next, the frequency properties of DCI factors deal with the dimensionless values which are divided the DCI factors values by f_{11} value when $l/a = \infty$, $\omega/\omega g = 0.0$.

NUMERIC RESULTS AND CONCLUSION

In this paper, by varying the separation ratio l/a, the embedded ratio a/H and the location of two structures relative to the input motion direction φ shown in Fig. 1, many numerical calculations were done for identical two rigid structures. Fig. 3 and 4 show the curve of f_{11}, f_{13} and g_1 versus with l/a and the frequency ratio $\omega/\omega g$ when $a/H = 1.0$, $\varphi = 0°$. In the case of $a/H = 1.0$ and $l/a = 3.0$, the curves of [F] and {G}, in which f_{12}, f_{14} and g_2 are the cross factors whose values are zero as $\varphi = 0°$ or $90°$, are shown in Fig. 5 and 6. The dynamic magnification factor MF at the center of gravity of structure versus with a/H and $\omega/\omega g$ are plotted in Fig. 7 when $\varphi = 0°$ and $\omega_R/\omega g = 1.5$. Where ω_R denotes the natural frequency of rocking motion of structure. Fig. 8 shows the curves by plotting the largest values of MF versus with l/a and $\omega_R/\omega g$ when the value of MF has a maximum near $\omega = \omega_R$ (in the case of a/H = 1.0 as shown in Fig. 7), while Fig. 9 shows the curves when the value has a maximum near $\omega = \omega g$ (in the case of a/H = 0.25). The curves of MF versus with φ and $\omega/\omega g$ are shown in Fig. 10 when a/H = 1.0, l/a = 3.0 and $\omega_R / \omega g = 1.5$.

From the numeric results the effects of DCI are obtained as follows;
1) when $\varphi = 0°$, the amplification of the rigid structure increases near $\omega = \omega_R$ while decreases $\omega = \omega g$ in comparison with the single body problem ($l/a = \infty$). This tendency becomes more remarkable the more two structures located near. 2) When φ is not equal to 0° or 90°, the rocking direction of structure does not agree with the direction of input ground motion (x-direction), because the response components in y-direction are induced. And the y-direction components become a maximum when $\varphi = 45°$.

REFERENCES

1) T. Inukai, K. Miura, T. Nishikawa and S. Terada, "Dynamic characteristics of Cross Interaction of Two Embedded Structures through Elastic Surface Layer," Annual Meeting Reports of Kanto Branch of A.I.J., Vol. 49, pp. 109-112, 1978. (in Japanese)
2) H. Tajimi, "Dynamic Analysis of a Structure Embedded in an Elastic Stratum," Proc. 4th W.C.E.E., pp. 54-69, 1969
3) T. Kobori, R. Minai and K. Kusakabe, "Dynamical Characteristics of Soil-Structure Cross Interaction," Bull. Disas. Prev. Res. Inst. of Kyoto Univ., Vol. 22, No. 204, 1973
4) K. Miura, S. Terada and T. Tajime, "Dynamic Characteristics of Embedded Rigid Structure with Rectangular Cross Section," Memoirs of Faculty of Tech. Tokyo Metropolitan Univ., No. 26, pp. 91-106, 1976

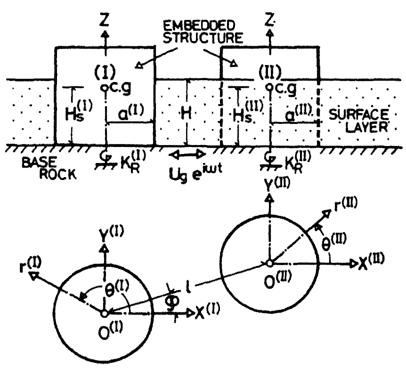

Fig. 1 Analytical Model of Cross Interaction

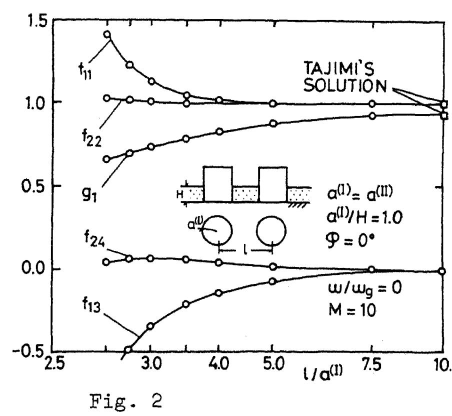

Fig. 2

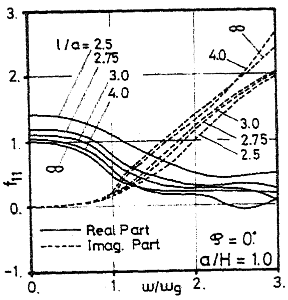

Fig. 3-(a)

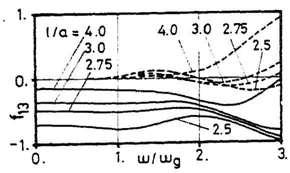

Fig. 3-(b)

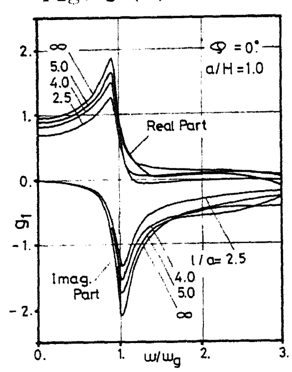

Fig. 4

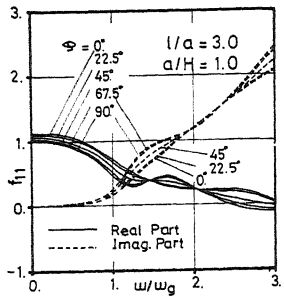

Fig. 5-(a)

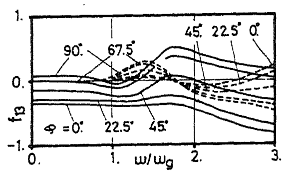

Fig. 5-(b)

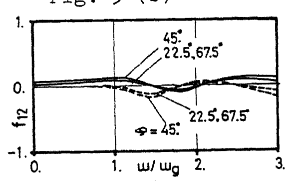

Fig. 5-(c)

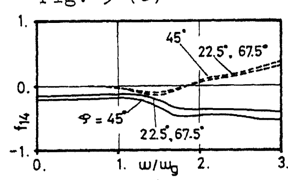

Fig. 5-(d)

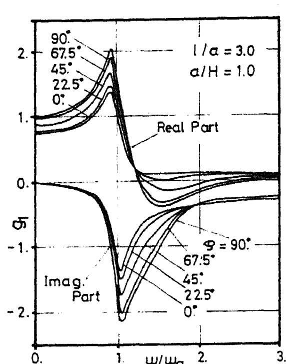

Fig. 6-(a)

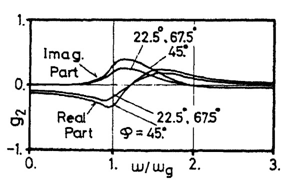

Fig. 6-(b)

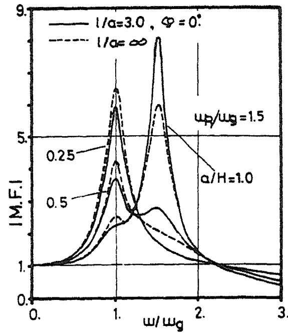

Fig. 7

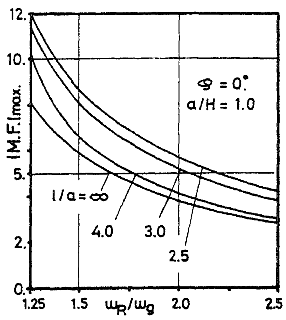

Fig. 8

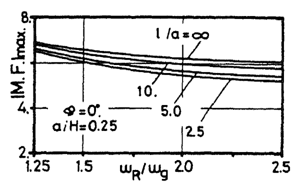

Fig. 9

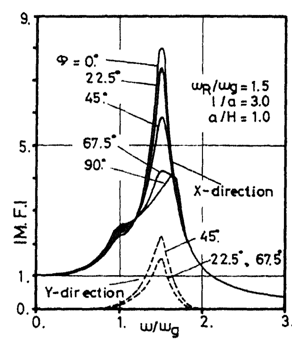

Fig. 10